

FIGURE 1.4. Some orbital characteristics. The Sun (S) is located at one of the two foci of the asteroid's elliptical orbit. Half the long, or major, axis of the ellipse is termed the semi-major axis (CP). The ratio of the distances CS to CP is the orbital eccentricity. The perihelion distance (SP) is usually denoted as "q" while the aphelion distance (SA) is denoted "Q."

TABLE 1.1. *Definitions of near-Earth objects*

Asteroid	A relatively small, inactive, (usually) rocky body orbiting the Sun
Comet	A relatively small, at times active object whose ices can vaporize in sunlight, forming an atmosphere (coma) of dust and gas and, sometimes, tails of dust and gas
Meteoroid	A small particle from a comet or asteroid that is orbiting the Sun and is less than one meter in extent
Meteor	The atmospheric light phenomenon that results when a meteoroid enters the Earth's atmosphere and vaporizes
Fireball	An event that is brighter than a meteor ranging in brightness from just brighter than the brightest planets to approaching the brightness of the Sun
Meteorite	A meteoroid that survives its passage through the Earth's atmosphere and lands upon the Earth's surface
Near-Earth Object	A comet or asteroid that can approach the Sun to within 1.3 AU. In order for a body to be classified as a near-Earth object, it must have an orbital period less than 200 years
Potentially Hazardous Object	A comet or asteroid that can approach the Earth's orbit within 0.05 AU or about 7.5 million kilometers and is large enough to cause impact damage

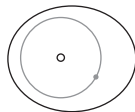
**Near Earth  
Object**

**Orbit Classes**

**Orbit Criteria**

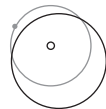
Amors

Earth approaching asteroids with orbits exterior to Earth's but interior to the orbit of Mars. Hence their semi-major axes are larger than 1.0 AU and their perihelia are between 1.017 and 1.3 AU.



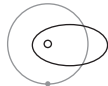
Apollos

Earth orbit crossing asteroids with semi-major axes larger than Earth's ( $a$  is larger than 1.0 AU) and with perihelia less than 1.017 AU.



Atens

Earth orbit crossing asteroids with their semi-major axes smaller than Earth's and their aphelia larger than 0.983 AU.



Atras

Asteroids with their orbits contained entirely within that of the Earth. Hence their semi-major axes are less than 1 AU and their aphelia are less than 0.983 AU.



FIGURE 1.5. The four heliocentric orbit classifications for the near-Earth asteroids.

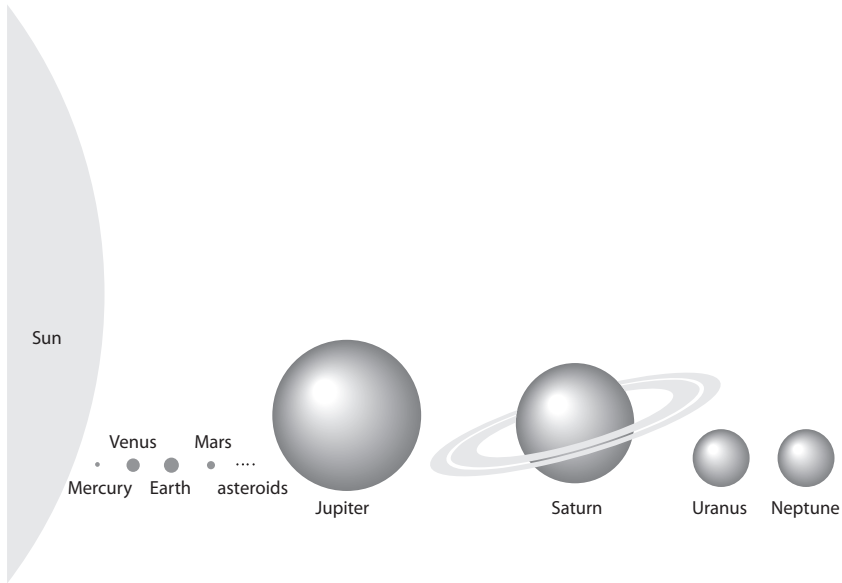


FIGURE 2.1. The eight major planets range in size from the smallest, most interior planet, Mercury, with a diameter of 4,879 kilometers to the largest, Jupiter, whose equatorial diameter is more than twenty-nine times Mercury's size with a diameter of about 143,000 kilometers. For comparison, the Earth's equatorial diameter is 12,756 kilometers. The approximate relative sizes of the planets are evident but the distances between the planets are not to scale.

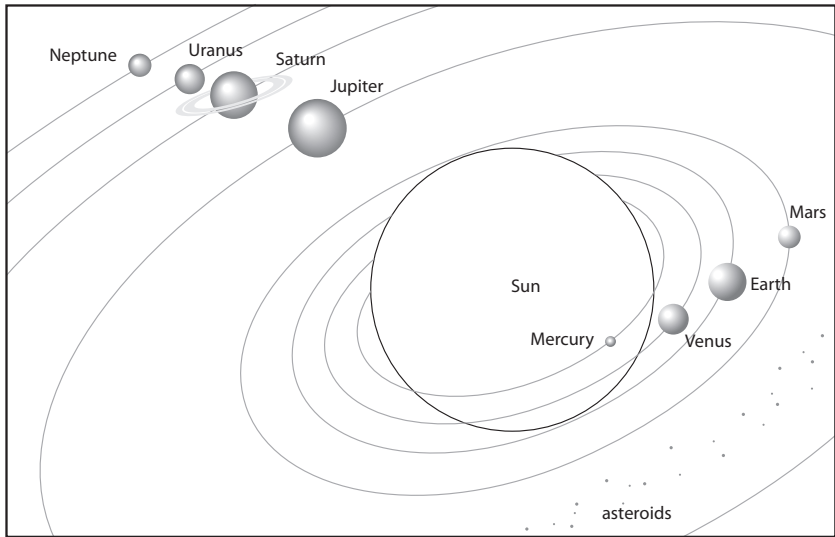


FIGURE 2.2. This schematic illustration shows the rough distances of the eight planets from the Sun. The respective semi-major axes of Mercury, Venus, Earth, Mars, Jupiter, Saturn, Uranus, and Neptune are 0.4, 0.7, 1.0, 1.5, 5.2, 9.5, 19.2, and 30.1 AU.

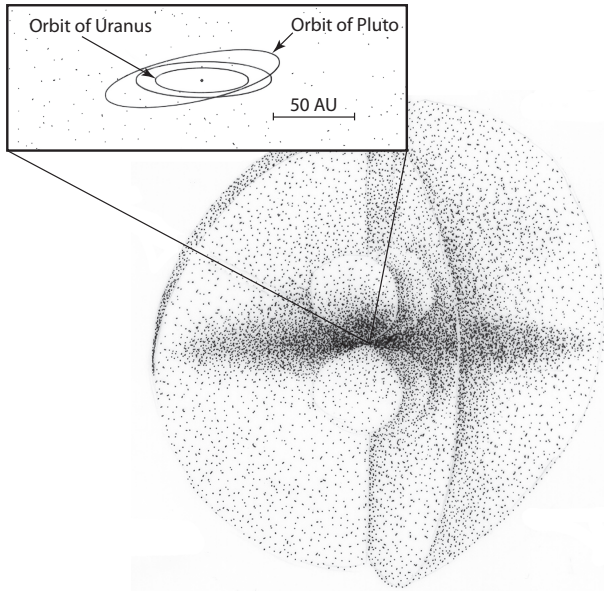


FIGURE 2.3. The Kuiper belt, a relatively flattened distribution of comet-like bodies, is located beyond the orbit of our outermost planet, Neptune, and extends to about 50 AU from the Sun. The dwarf planet Pluto is one of the largest members of the Kuiper belt. The scattered disk of comet-like objects is far less flattened than the Kuiper belt and extends out to 300 AU or more. One hundred billion comets reside in the Oort cloud, the outer edge of which at about 100,000 AU marks the distant boundary of our solar system where the Sun's gravity can no longer hold onto an Oort cloud comet.

TABLE 2.1. Distances from the Sun and relative masses for the planets, Pluto, and the solar system's small bodies

Body	Approximate distance from the Sun (in AU)	Mass (in units of the Earth's mass)
Sun	0	333,000
Mercury	0.39	0.055
Venus	0.72	0.815
Earth	1.0	1.0
Moon	1.0	0.012
Mars	1.52	0.107
Main asteroid belt	2–4	$6 \times 10^{-4}$
Jupiter	5.20	317.83
Jupiter Trojans	5.2	$10^{-5}$
Saturn	9.54	95.16
Uranus	19.18	14.54
Neptune	30.06	17.15
Pluto	39.47	0.002
Kuiper belt	35–50	<0.1
Oort cloud	1,000–100,000	4–80

*Note:* The Sun's mass is  $1.99 \times 10^{30}$  kg and that of the Earth is  $5.97 \times 10^{24}$  kg.

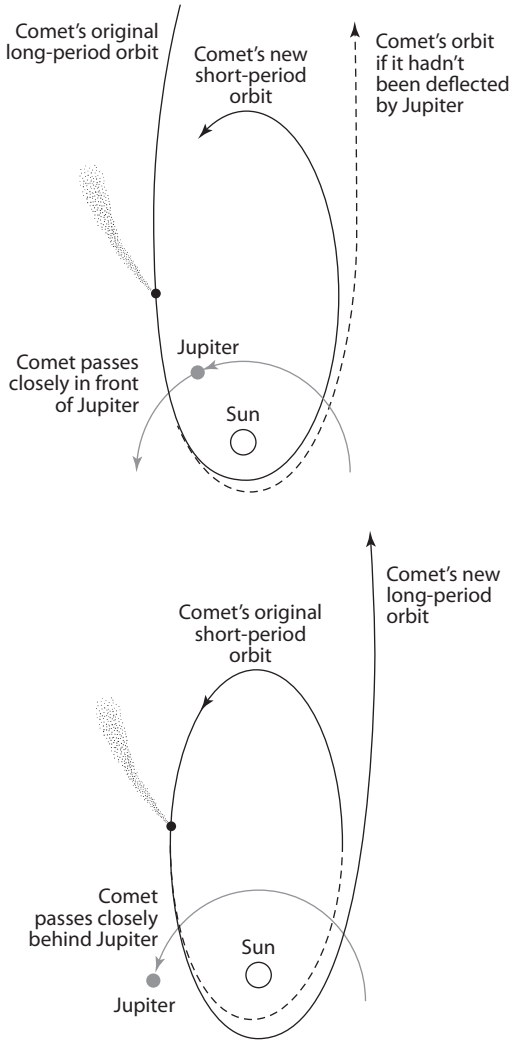


FIGURE 3.1. The passage of a comet or an asteroid past a planet will alter its future orbit, either removing orbital energy (reducing its orbital period) with a front-side passage of a planet or adding orbital energy (increasing its orbital period) with a trailing edge passage. For example, in the top frame, a comet makes a front-side passage of the planet Jupiter, loses orbital energy, and enters into an orbit with a shorter orbital period than before the Jupiter approach. In the bottom frame, the comet passes behind the planet Jupiter, gains orbital energy, and has its orbital period increased as a result. Space mission planners often take advantage of these planetary gravity assists to save rocket fuel when sending spacecraft to distant locations within the solar system.



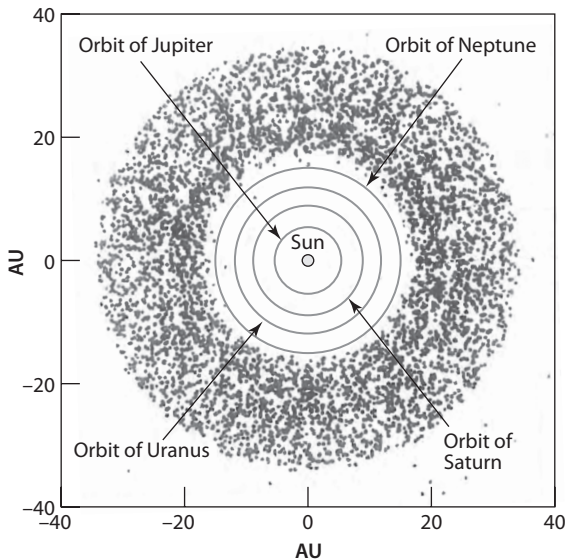


FIGURE 3.2. In one possible variant of the Nice model for the solar system's origin, the outer planets Jupiter, Saturn, Uranus, and Neptune began not on their current orbits but on nearly circular orbits at respective heliocentric distances of 5.5, 8.2, 11.5, and 14.2 AU. The model assumes that there was an initial dense region of planetesimals just outside the distance of the outermost planet, Neptune, which extended from about 15.5 to 34 AU. Over hundreds of millions of years as a result of interactions between the planets with one another and with the planetesimals, Jupiter moved a bit sunward to its current orbital position while Saturn, Uranus, and Neptune moved outward to their current orbits. In the planetary migration process, 99 percent of the original planetesimals were scattered away from their initial orbital locations.

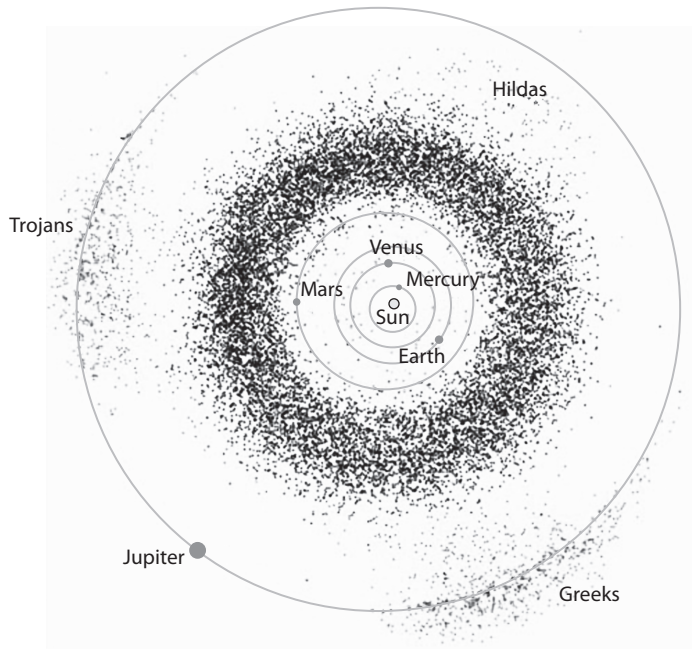


FIGURE 3.3. This current configuration diagram for the inner solar system shows the main belt of asteroids between the orbits of Mars and Jupiter, the so-called Trojan asteroids that lead (“Greeks”) and follow (“Trojans”) Jupiter by an average of 60 degrees and the Hilda-class of asteroids that have orbital periods two-thirds that of Jupiter. At their aphelia, the Hildas are either on the other side of the Sun from Jupiter’s position or near, but slightly inside, the Trojan asteroid locations so they, like the Trojans themselves, avoid the strong gravitational perturbations by Jupiter.

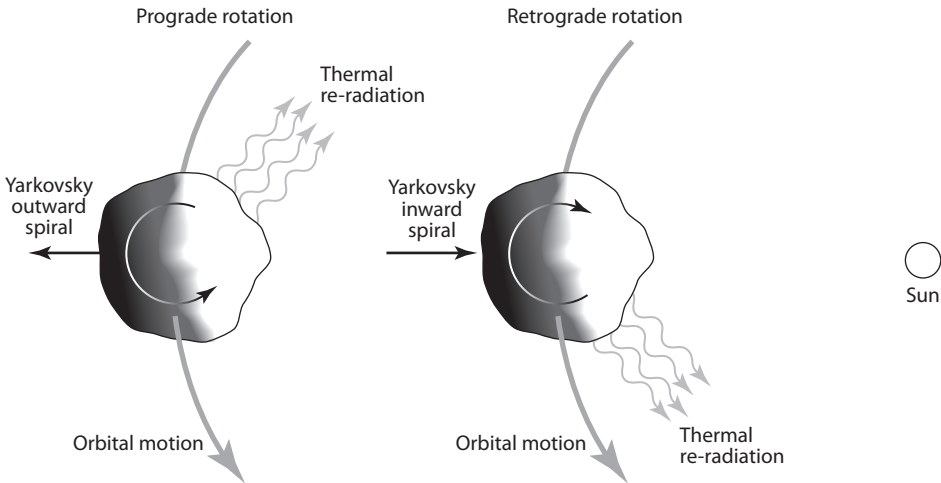


FIGURE 3.4. The so-called Yarkovsky force affects the long-term motion of relatively small asteroids due to a time lag between when sunlight is received upon the surface of the asteroid and when it is re-radiated. Because the asteroid is rotating, there is a small but non-negligible thrust in a direction somewhat different than the Sun's direction. Hence there is a tiny push on the asteroid either in the direction of its orbital motion if the rotation is in the same sense as its motion about the Sun (prograde or direct rotation) or counter to its orbital motion if its rotation is in the opposite sense (retrograde). As shown in the illustration, a prograde rotation will result in energy being added to the asteroid's orbit with a subsequent outward spiral and an increase in the orbital period. A retrograde rotation will subtract orbital energy and decrease the orbital period.

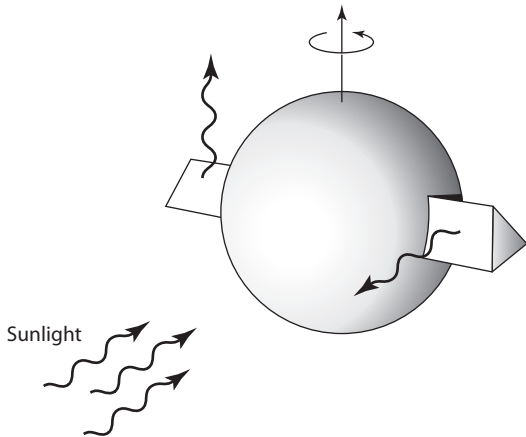


FIGURE 3.5. The YORP effect. As a result of uneven re-radiation of solar energy from one side of a rotating asteroid with respect to the other side, the re-radiation of thermal energy to space can act to increase or decrease the asteroid's rotation rate.



FIGURE 4.2. Map showing Chicxulub crater area on the edge of the Mexican Yucatán peninsula.

**Known Near-Earth Asteroids**  
January 1980 through August 2011

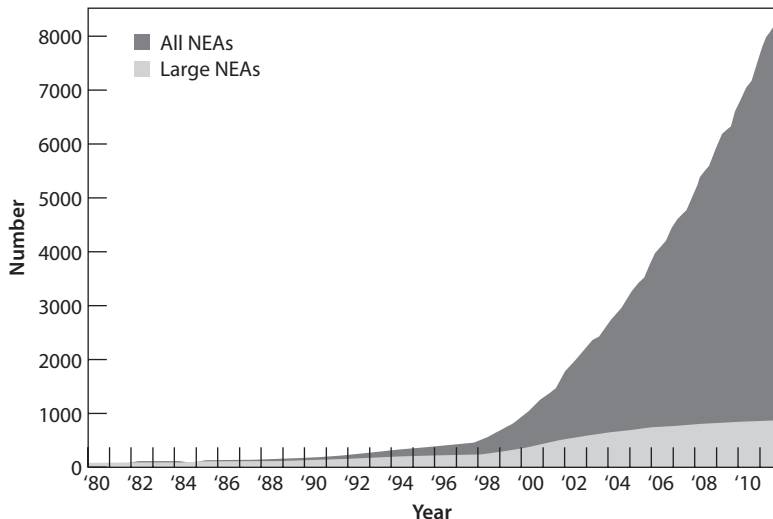


FIGURE 5.6. Plot showing the rapid increase in near-Earth asteroid discoveries in the late 1990s and beyond. The darker curve shows the number of discoveries of near-Earth asteroids of all sizes versus date while the lighter curve shows the number of discoveries of one-kilometer and larger near-Earth asteroids versus date.

Source: Courtesy of Alan Chamberlin, NASA/JPL-Caltech.

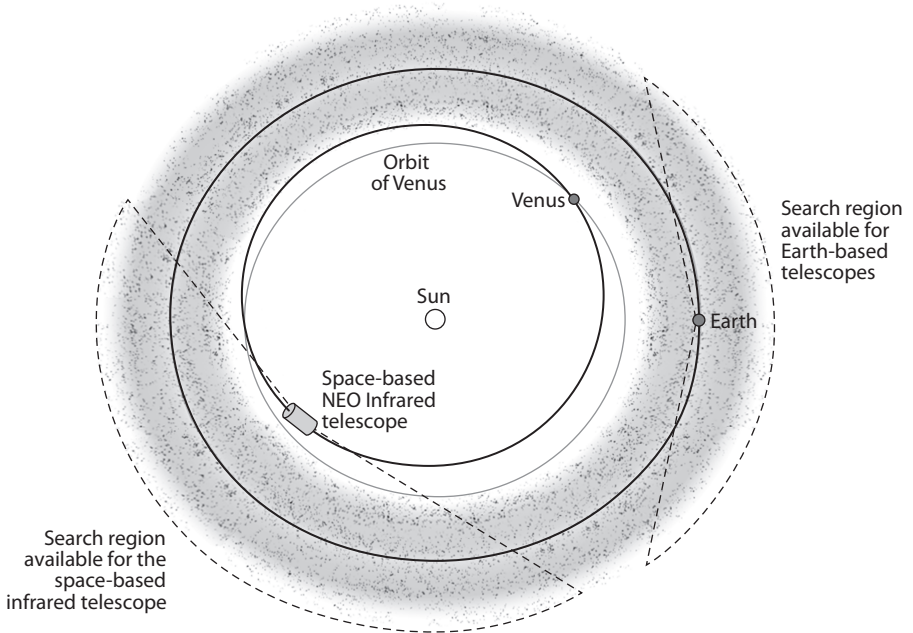


FIGURE 5.7. This diagram shows the advantage a space-based infrared telescope would have over Earth-based optical telescopes for discovering near-Earth asteroids. The nominal search region available from Earth is shown, where Earth is located at the 3 o'clock position. This search region should be compared to the much larger region available from an NEO infrared telescope located at the 8 o'clock position on an orbit similar to that of the planet Venus, interior to the Earth's orbit about the Sun. In addition, when compared to optical telescopes on Earth, this space-based infrared telescope would more easily see dark near-Earth asteroids, would circulate around the Sun more rapidly than the Earth, could operate twenty-four hours per day, and would have less confusion from the background stars.

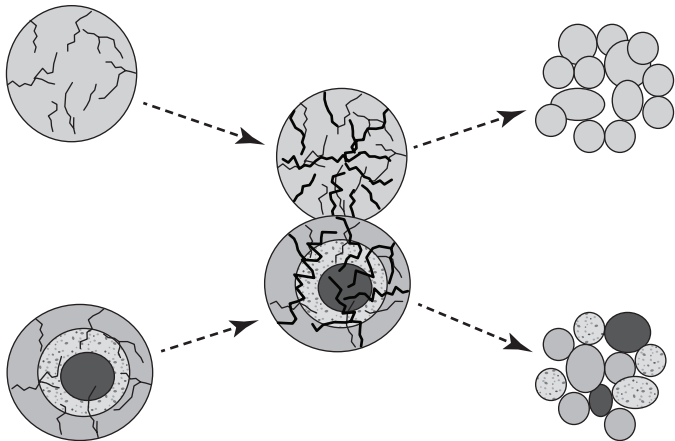


FIGURE 6.1. Cartoon showing the origin of different asteroid types and the meteorites that can arrive on Earth from these asteroids. A differentiated, or layered, asteroid could collide with an undifferentiated, or unlayered, rocky silicate body, forming smaller asteroids and potential meteorites. The collision fragments can have the characteristics of the original rocky silicate object or of the various regions of the differentiated asteroid, including the loose top layer, the stony-iron nature of the middle region, or the iron-nickel metallic nature of the core region.



Rotation Period vs. Diameter  
2010, 3643 Asteroids

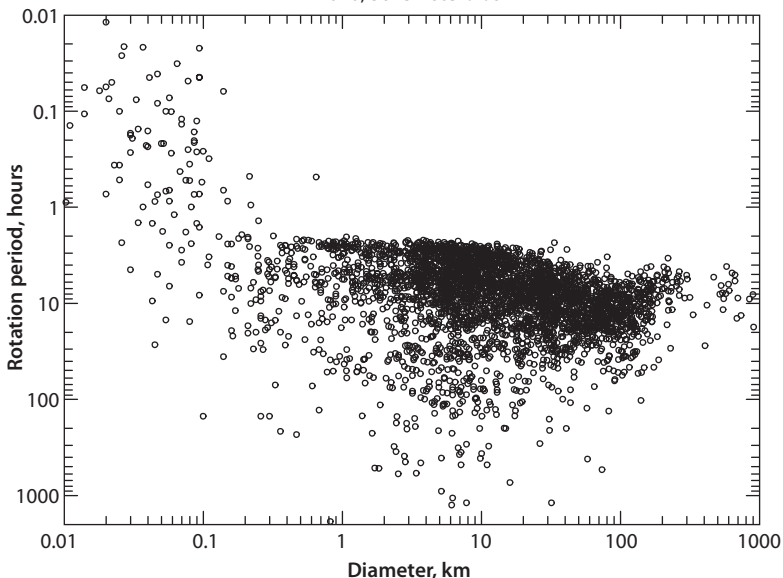


FIGURE 6.4. Plot of asteroid rotation periods versus size. Notice the paucity of asteroids larger than about 150 meters that have rotation periods less than two hours. Likewise, there are relatively few asteroids smaller than 150 meters that have rotation periods of greater than two hours.

Source: Courtesy of Alan W. Harris.

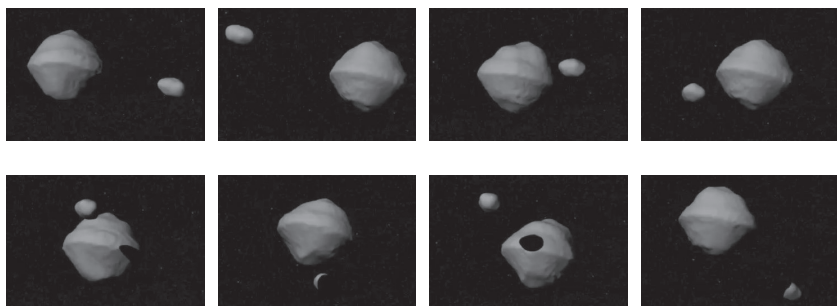


FIGURE 6.5. Radar observations of near-Earth asteroid (66391) 1999 KW4 taken in May 2001 revealed it to be a binary object with an equatorial bulge on the larger body. The longest dimension of the primary asteroid and its moon are 1.6 and 0.6 kilometers, respectively. The moon orbits the primary asteroid in about 17.4 hours at a distance of 2.5 kilometers.

Source: Courtesy of NASA/JPL-Caltech.

TABLE 6.1. Spacecraft observations of asteroids

For each spacecraft encounter with an asteroid, the best pixel scale, encounter time, and encounter distance are given.

Target Body	Best Pixel Scale (meters)	Mission Name	Encounter Arrival or Flyby Date	Distance (kilometers)
Gaspra	54	Galileo <sup>1</sup>	10/29/1991	1,600
Ida/Dactyl	30	Galileo	08/28/1993	2,391
Mathilde	160	NEAR <sup>2</sup>	06/27/1997	1,212
Eros	0.05	NEAR	02/12/2000	Rendezvous & Landing
Braille <sup>3</sup>	120	DS1	07/29/1999	28
Annefrank <sup>4</sup>	185	Stardust	11/02/2002	3,079
Steins	80	Rosetta <sup>5</sup>	09/05/2008	803
Lutetia	60	Rosetta	07/10/2010	3,162
Itokawa	0.06	Hayabusa <sup>6</sup>	09/2005	Rendezvous & Landing
Vesta	20	DAWN <sup>7</sup>	07/2011	Rendezvous
Ceres	70	DAWN	02/2015	Rendezvous

<sup>1</sup> The Galileo spacecraft flew past asteroid (951) Gaspra and (243) Ida. The longest dimensions of Gaspra and Ida are 19 and 54 km, respectively, and a 1.6-km-sized moon (Dactyl) was discovered orbiting Ida. Dactyl was the first of many asteroid moons to be discovered.

<sup>2</sup> The Near-Earth Asteroid Rendezvous (NEAR) mission discovered four large craters on (253) Mathilde that are comparable in diameter to the asteroid's radius. The NEAR Shoemaker spacecraft spent about a year in orbit about near-Earth object (433) Eros before the spacecraft was boldly landed on the asteroid's surface. Mathilde is roughly spherical with a longest dimension of 66 km while Eros is shaped a bit like a fat sausage with a longest dimension of 34 km.

<sup>3</sup> (9969) Braille, about 2 km in its longest dimension, has a long rotation period of 226 hours. While the close approach distance was only 28 km, this object was imaged at a distance of 13,500 km by the Deep Space 1 spacecraft.

<sup>4</sup> Asteroid (5535) Annefrank has a roughly ellipsoidal shape with a longest dimension of 6.6 km.

<sup>5</sup> The European Space Agency's Rosetta spacecraft, on its journey to comet Churyumov-Gerasimenko, flew past asteroids (2867) Steins and (21) Lutetia. Steins is about 6.7 km in its longest dimension and was imaged with both the narrow-angle and wide-angle cameras, but a shutter problem on the narrow-angle camera prevented images from that instrument near its closest approach. Lutetia's long dimension is about 130 km.

<sup>6</sup> On two occasions in November 2005, the Hayabusa spacecraft touched down on the surface of near-Earth asteroid (25143) Itokawa. Although the spacecraft sampling mechanism failed during each touchdown attempt, dust particles stirred up by contact with the surface were captured and brought back to Earth on June 13, 2010.

<sup>7</sup> The DAWN spacecraft carried out a rendezvous with asteroid (4) Vesta in July 2011, and there are plans to carry out a rendezvous with dwarf planet Ceres in 2015.

TABLE 6.2. Spacecraft observations of comets

For each spacecraft encounter with a comet, the best pixel scale, encounter time, and encounter distance are given.

Target Body	Best Pixel Scale (meters)	Mission Name	Arrival or Flyby Date	Encounter Distance (kilometers)
Giacobini-Zinner		ICE <sup>1</sup>	9/11/1985	7,800
Halley		VEGA 1 <sup>2</sup>	03/06/1986	8,890
		Suisei <sup>3</sup>	03/08/1986	150,000
		VEGA 2	03/09/1986	8,030
		Sakigake	03/11/1986	7 million
	45	Giotto <sup>4</sup>	03/14/1986	596
Borrelly	47	DS1 <sup>5</sup>	09/22/2001	2,171
Wild 2	15	Stardust <sup>6</sup>	01/02/2004	240
Tempel 1	1	Deep Impact <sup>7</sup>	07/04/2005	500
Hartley 2 <sup>8</sup>	4	Deep Impact	11/04/2010	700
Tempel 1 <sup>9</sup>	10	Stardust-NExT	02/15/2011	178
Churyumov-Gerasimenko		Rosetta <sup>10</sup>	mid-2014	

<sup>1</sup> The International Cometary Explorer (ICE) spacecraft passed 21P/Giacobini-Zinner on the side away from the sun about 7,800 km from its nucleus. It carried no camera but did detect the magnetic field of the sun wrapped around the comet's ion atmosphere. Earlier in its career, the ICE spacecraft was used to study the interaction of the solar wind particles with the Earth's charged particle and magnetic field environment from a point between the Sun and Earth. After four years of these observations, a series of five lunar gravity assists designed by Robert Farquhar were carried out and the International-Sun-Earth-Explorer 3 (ISEE-3) spacecraft was then retargeted (and renamed ICE) for a flyby of comet Giacobini-Zinner.

<sup>2</sup> The Soviet Union sent two spacecraft to comet 1P/Halley. The camera on the VEGA 1 spacecraft was somewhat out of focus and the camera on the VEGA 2 spacecraft obtained overexposed images of the comet's nucleus. Comet Halley's longest dimension is about 15 km.

<sup>3</sup> Japan's Suisei and Sakigake spacecraft were designed to study the solar wind interaction with the comet's atmosphere. Neither spacecraft carried a camera.

<sup>4</sup> The European Space Agency's Giotto spacecraft was programmed to image the brightest object in its field of view, so the highest-resolution nucleus images were located adjacent to a bright dust jet.

<sup>5</sup> The Deep Space 1 (DS1) spacecraft, designed to test new technologies including an ion drive engine, flew past comet 19P/Borrelly and used its camera to provide images of an elongated bowling pin-shaped nucleus whose longest dimension was about 8.4 km. The highest resolution image was taken at a distance of 3,556 km.

<sup>6</sup> The Stardust spacecraft collected cometary dust samples during the flyby of 81P/Wild 2 and returned them to Earth for study on January 15, 2006. The longest axis of this roughly spherical nucleus is about 5.5 km. The main Stardust spacecraft, now renamed Stardust-NExT, was retargeted for a flyby of comet 9P/Tempel 1 on February 15, 2011. "NExT" was added to the mission name to denote "New Exploration of Tempel 1."

(continued)

TABLE 6.2. *Continued*

---

<sup>7</sup> Comet 9P/Tempel 1 was observed from the flyby spacecraft from a distance of about 700 km. The spacecraft then stopped imaging and switched to “shield mode” to mitigate near-nucleus dust hits. The impactor spacecraft was able to take high-resolution images and radio them back to the flyby spacecraft before vaporizing during the impact itself. This comet’s nucleus is sort of a rounded pyramid with a longest dimension of 7.6 km.

<sup>8</sup> After its flyby of comet Tempel 1 in July 2005, the Deep Impact spacecraft was retargeted for a flyby of comet Hartley 2 in November 2010. The nucleus of comet 103P/Hartley 2 was a bizarre sight to see. It is shaped like an elongated peanut, 2.3 km in its longest dimension and with a smooth neck connecting two larger end members that were very rough.

<sup>9</sup> The nucleus of comet 9P/Tempel 1 was observed in July 2005 by the Deep Impact spacecraft and again in February 2011 by the Stardust-NExT spacecraft. The February 2011 observations identified the impact crater created by the 2005 Deep Impact mission. The crater was about 50 meters in diameter but quite indistinct and subdued with a raised central mound, suggesting that the nucleus has a fragile and porous surface.

<sup>10</sup> The European Space Agency’s Rosetta mission will rendezvous with comet 67P/Churyumov-Gerasimenko in mid-2014, observe the active nucleus for several weeks through perihelion, and deploy a lander to closely investigate the surface of the nucleus. If successful, the nucleus lander could achieve a pixel scale of 2 centimeters per pixel.

TABLE 8.1. Average impact results, by size

Diameter of Impactor <sup>1</sup>	Total NEA Population <sup>2</sup>	Typical Impact Energy <sup>3</sup>	Average Interval between Impacts	Crater Diameter
1m	1 billion	47 (8) tons	2 weeks	No crater
10 m	10 million	47 (19) KT	10 years	No crater
30 m	1.3 million	1.3 (0.9) MT	200 years	No crater
100 m	20,500–36,000	47 (4) MT	5,200 years	1.2 km
140 m	13,000–20,000	129 (49) MT	13,000 years	2.2 km
500 m	2,400–3,300	5,870 (5,610) MT	130,000 years	7.4 km
1 km	980–1,000	47,000 (46,300) MT	440,000 years	13.6 km
10 km	4	47 million MT	89 million years	104 km

<sup>1</sup> The smallest-diameter, stony, near-Earth asteroid that will reach the ground with at least half its original energy is about 160 meters. The diameter of the smallest rocky asteroid that can cause significant ground damage is in the range of 30 to 50 meters, roughly the size of the Tunguska impactor that fell in June 1908.

<sup>2</sup> The total near-Earth asteroid (NEA) population estimates, especially at the smaller sizes, are quite uncertain. For the objects whose diameters are about 100 meters, 140 meters, 500 meters, and 1 kilometer, the lower number was estimated using the NEOWISE infrared observations and the higher number was determined using the optical observations.

<sup>3</sup> For each size of impactor in the table, the first energy value given represents the total energy lost to the Earth’s atmosphere and surrendered as a result of the final airburst or Earth impact. In each case, the energy value given in parentheses is the airburst or impact energy by itself. For example, for an impactor with an initial diameter of 140 meters, the total collision energy would be equivalent to 129 million tons (129 megatons) of TNT explosives, but 80 megatons of this energy would be lost due to the object fragmenting and heating the atmosphere during its flight path. That would leave 49 megatons for the final Earth impact itself.

TABLE 8.2. The average number of fatalities per year worldwide from various accidents, events, and illnesses, compared to the estimated 100 annual fatalities for near-Earth object collisions

Threat	Estimated Fatalities per Year
Shark attacks	3–7
Asteroids	91
Earthquakes	36,000
Malaria	1 million
Traffic accidents	1.2 million
Air pollution	2 million
HIV/AIDS	2.1 million
Tobacco	5 million

*Note:* The estimate of 91 annual deaths is worse than that for shark attacks and about comparable to that of accidents due to fireworks. On the other hand, fireworks do not have the capacity to reduce large regions of the Earth’s surface to ashes and create another extinction event. Comparisons like those in this table are a bit misleading because near-Earth asteroid impacts are very low-probability—but very high-consequence—events. Obviously 91 people do not die each year from asteroid impacts; this is a long-term average arising from very catastrophic events occurring only rarely.

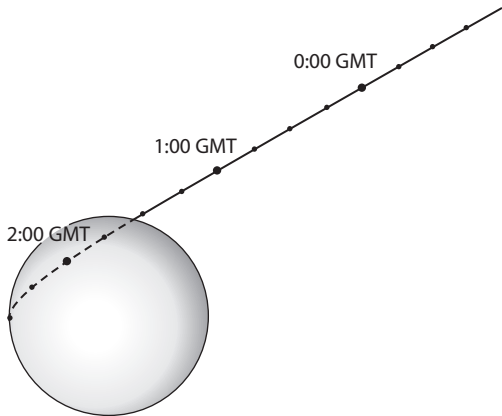


FIGURE 9.1. The terminal trajectory for Earth-impacting asteroid 2008 TC3. The view is from the Sun. Note that the asteroid entered Earth's shadow at about 1:49 AM Greenwich time on October 7, 2008 (8:49 PM EST on October 6), so that the final portion of the trajectory is in shadow behind the Earth.

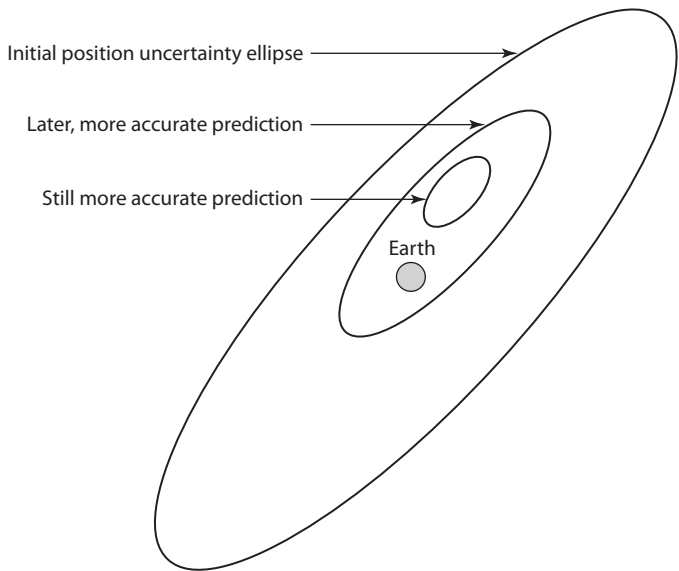


FIGURE 9.2. The Earth's target plane diagram. At the time of a close-Earth approach, an object's position uncertainty ellipsoid, when projected on a plane perpendicular to the incoming trajectory, becomes an uncertainty ellipse, and if any portion of this ellipse should touch or include the Earth's capture cross section, there will be a chance of an Earth impact. An object's uncertain initial orbit will provide uncertain future predictions for its position during a close-Earth approach. Then its relatively large initial uncertainty ellipse could include the Earth and an impact could not be ruled out. However, the object's future position predictions improve as more observations are included in the orbit updates: the object's uncertainty ellipse at the time of the close-Earth approach would then shrink and, almost always, subsequent orbit updates would completely rule out an Earth collision.



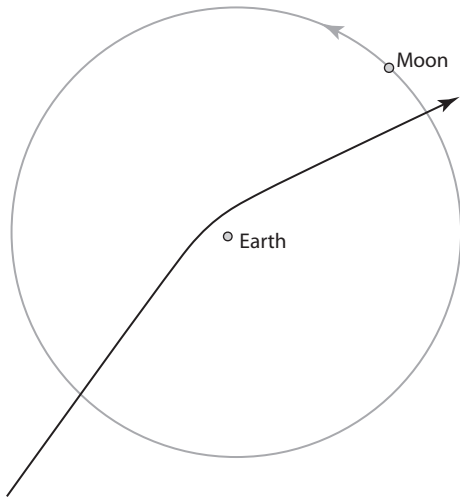


FIGURE 9.3. (99942) Apophis flies by Earth on April 13, 2029. The most likely trajectory of Apophis is shown as a curved line that passes near the Earth on April 13, 2029. The collection of possible Apophis orbits that make up its position uncertainty ellipsoid do not reach the Earth's capture cross section so no Earth impact is possible in 2029.

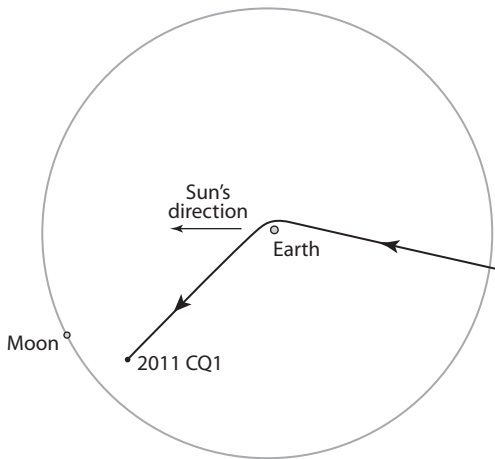


FIGURE 9.4. Near-Earth asteroid 2011 CQ1, a one-meter-sized asteroid, flew within 0.85 Earth radii of the Earth's surface on February 4, 2011. The Earth's gravitational attraction bent its orbit by 68 degrees before the asteroid resumed its journey about the Sun.



FIGURE 10.2. An example of the so-called risk corridor for a near-Earth asteroid. For an asteroid that has a remote chance of striking Earth, the highly elongated uncertainty ellipsoid region of its orbital position, when projected upon the Earth's surface, forms a narrow "risk corridor" that can wrap nearly around the entire Earth. If the asteroid should actually hit the Earth, it would do so somewhere along this risk corridor.